

# Optical sensing for real-time blood monitoring in extracorporeal circulation: Performance assessment of a biocompatible sensor and off-label investigation of a commercial device

Alessia Gallerani<sup>1,2</sup>, Marco Muzzarelli<sup>1</sup>, Alberto Ferrari<sup>2</sup>, Stefano Cattini<sup>1</sup>, Luigi Rovati<sup>1,2</sup>

<sup>1</sup> "Enzo Ferrari" Department of Engineering, University of Modena and Reggio Emilia, Modena, Italy

<sup>2</sup> Science & Technology Park for Medicine, TPM, Mirandola, Modena, Italy

## ABSTRACT

Continuous monitoring of blood pCO<sub>2</sub> is critical during extracorporeal circulation (ECC) to support clinical decision-making. This study aims to describe and investigate a new, low-cost, disposable fluorescent pCO<sub>2</sub> sensor, namely MS2. The performance of MS2 is analysed by comparison with a blood gas analyzer. A significant challenge in developing sensors for *in vivo* applications is ensuring biocompatibility. In the MS2 sensor, biocompatibility is ensured by using a medical-grade gas-permeable membrane that isolates the sensing chemistry from the patient's blood.

The study also investigates the performance of a commercial optical pCO<sub>2</sub> sensor, the PreSens MCR-O1P1C1, which is not approved for use with blood. The aim is to assess the feasibility of employing the PreSens MCR-O1P1C1 for blood monitoring in scenarios where biocompatibility is not a prerequisite, such as in the development stages of biomedical devices that require *ex vivo* blood testing.

The results obtained during a 6.5-hour test with bovine blood demonstrate that both measuring systems can provide valid support for monitoring pCO<sub>2</sub> in blood. However, despite its excellent response times, the off-label application of the PreSens MCR-O1P1C1 necessitates an adjustment of the measuring system to prevent significant measurement errors. Thus, these results position MS2 as a promising solution for real-time, in-line blood gas monitoring in ECC procedures.

## Section: RESEARCH PAPER

**Keywords:** blood pCO<sub>2</sub>, biomedical monitoring, biomedical measurement, optical sensors, extracorporeal circulation (ECC), hemodialysis, extracorporeal membrane oxygenation (ECMO), extracorporeal carbon dioxide removal (ECCO2R), heart lung machine, severe acute respiratory syndrome (SARS)

**Citation:** A. Gallerani, M. Muzzarelli, A. Ferrari, S. Cattini, L. Rovati, Optical sensing for real-time blood monitoring in extracorporeal circulation: Performance assessment of a biocompatible sensor and off-label investigation of a commercial device, Acta IMEKO, vol. 15 (2026) no. 2, pp. 1–8. DOI: [10.21014/actaimeko.v15i2.2263](https://doi.org/10.21014/actaimeko.v15i2.2263)

**Section Editor:** Maik Rosenberger, Ilmenau University of Technology, Germany

**Received:** December 4, 2025; **In Final Form:** June 18, 2026; **Published:** June, 2026.

**Copyright:** This is an open-access article distributed under the terms of the [Creative Commons Attribution 4.0 International License](https://creativecommons.org/licenses/by/4.0/).

**Funding:** No funding specified.

**Corresponding Author:** Alessia Gallerani, e-mail: [alessia.gallerani@unimore.it](mailto:alessia.gallerani@unimore.it)

## 1. INTRODUCTION

Continuous and accurate monitoring of critical care analytes — including blood electrolytes, metabolites, and blood gases such as oxygen (O<sub>2</sub>) and carbon dioxide (CO<sub>2</sub>) — is essential during extracorporeal blood circulation (ECC) procedures. Such monitoring plays a crucial role in the diagnosis and treatment of severe health disorders. Among these analytes, the partial pressure of carbon dioxide (pCO<sub>2</sub>) is of particular interest due to its direct involvement in acid-base balance, respiratory function, and oxygen transport regulation. Carbon dioxide is a byproduct of cellular metabolism and exists in blood in three forms: dissolved CO<sub>2</sub>, carbonic acid (H<sub>2</sub>CO<sub>3</sub>), and bicarbonate ions (HCO<sub>3</sub><sup>-</sup>). These forms contribute to the regulation of blood pH, which is normally maintained within a narrow physiological range between [7.35, 7.45]. In clinical contexts, the pCO<sub>2</sub> physiological range

must remain between [35, 45] mmHg; deviations from normal levels can lead to severe clinical conditions such as hypercapnia (elevated pCO<sub>2</sub>) or hypocapnia (reduced pCO<sub>2</sub>), both of which are common in critically ill patients and may result in seizures, coma, or death [1]. Since under physiological conditions the body maintains a strict control on the blood pCO<sub>2</sub> to maintain it within a narrow range, real-time and in-line monitoring is critical during ECC procedures such as cardiopulmonary bypass, extracorporeal membrane oxygenation (ECMO), or extracorporeal CO<sub>2</sub> removal (ECCO2R). The measurement of pCO<sub>2</sub> is of significance across a wide range of domains, extending beyond clinical contexts. Consequently, a wide range of measurement methods have been devised over the years. Standard techniques employed for pCO<sub>2</sub> monitoring encompass electrochemical and optical methods, including fluorescence and optical absorption [2] [3] [4] [5].

However, to be suitable for continuous clinical use, the measuring devices must fulfill some mandatory requirements to ensure patient safety: the parts in direct contact with the patient must be biocompatible, sterilizable, non-toxic, and preferably disposable to prevent complications from post-use sterilization or cross-contamination. For blood  $p\text{CO}_2$  assessment, they must also meet strict metrological standards including an acceptable clinical error ( $\Delta p\text{CO}_2$ ) not exceeding  $\pm 5$  mmHg in the range [20, 100] mmHg for long treatments [6]. One of the major challenges in developing sensors for ECC systems is achieving full and sustained biocompatibility. Preventing direct exposure of blood to the sensing element enhances device safety, functionality, and long-term stability. Commercial systems like the Terumo CDI 550 Blood Parameter Monitoring System have been widely adopted during cardiopulmonary bypass procedures for their ability to continuously measure parameters such as pH,  $p\text{CO}_2$ ,  $p\text{O}_2$ , and electrolytes like potassium ( $\text{K}^+$ ), using optical fluorescence technologies integrated in-line within the ECC circuit [7]. In this work, we describe and investigate a new, low-cost, disposable fluorescent  $p\text{CO}_2$  sensor, referred to as the MS2 sensor. Our proposed system consists of a disposable sensing component, which comes into direct contact with blood, optically interrogated by an optical head that remains on the electromedical device. MS2 leverages hollow, porous, and hydrophobic polypropylene fibers — similar to those used in ECMO systems — to facilitate selective, bidirectional gas exchange between the blood and the measuring chamber housing the sensing element [8]. Since achieving biocompatibility is a major challenge in developing sensors for *in vivo* applications, fibers employed in MS2 allow efficient diffusion of  $\text{CO}_2$  while preventing direct blood contact with the sensing element, thereby ensuring safety, avoiding hemolytic or hemotoxic effects, and eliminating concerns about leachables. In parallel, this study evaluates the performance of a commercial optical  $p\text{CO}_2$  measuring system consisting of the PreSens optical multi-channel MCR-O1P1C1 and SP-CD1  $\text{CO}_2$  sensor spot. Although this device has been validated for use with biological fluids, it has not received regulatory approval for use with blood. Consequently, the present study investigates its performance in the context of off-label utilisation. The goal is to assess whether the PreSens system can be employed for blood monitoring in settings where biocompatibility is not required, such as during the development of biomedical devices that involve *ex vivo* blood testing. In both MS2 and PreSens system evaluations, a blood gas analyzer, considered as the current gold standard instrument for blood analytes monitoring in clinical contexts, served as the reference instrument.

## 2. METHODS AND PROCEDURES

In this section, we first present the working principle of the MS2 sensor (Section 2.1.), followed by a detailed description of its structural design (Section 2.2.). The mathematical model used for  $p\text{CO}_2$  estimation is then derived in Section 2.3.. In section 2.4., an overview of the PreSens sensor is provided. Finally, the experimental setup, including all relevant parameters and the configuration of the circulation circuit used during the measurement sessions, is described in Section 2.5..

### 2.1. Sensor working principle

The core of the proposed measuring system is based on the same principle used in oxygenators:  $\text{CO}_2$  exchange occurs across porous hollow fibers. The setup consists of a 20 mL polycarbonate cylinder (cuvette) packed with  $\approx 200$  fibers. Both ends of the cuvette are sealed using a potting procedure, which secures the

fibers, isolates their lumens from the external environment, and keeps them open. Two luer connectors provide access to the outer side of the fibers. During operation, blood flows through the fiber lumens, while the external compartment, hereinafter referred to as the measuring chamber, is filled with a pH-sensitive solution containing a ratiometric fluorophore and a phosphate buffer solution (PBS). Ratiometric fluorophores are chosen for their reliability in providing accurate measurements [9] [10]. Among these, we chose HPTS (8-hydroxypyrene-1,3,6-trisulfonic acid trisodium salt) because it is pH-sensitive, inexpensive, non-toxic, and photostable [11]. Figure 1 shows a picture of the fully assembled cuvette used during the test.

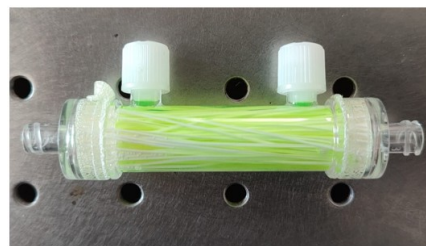


Figure 1. Picture of the disposable part of the MS2 sensor: a bundle of polypropylene hollow fibers is inserted inside the polycarbonate case. A potting procedure is performed on both sides of the case to separate the fibers' lumens from the external measuring chamber. The bright yellow color is due to the pH-sensitive solution containing HPTS and PBS.

Since fibers are gas-permeable,  $\text{CO}_2$  dissolved in blood diffuses through the fibers' walls into the external measuring chamber until an equilibrium condition in which the  $\text{CO}_2$  concentration ( $[\text{CO}_2]$ ) present in blood equals the one in the measuring chamber. The  $\text{CO}_2$  absorbed in the measuring chamber alters the pH of the sensitive solution and its fluorescent response. By detecting changes in the fluorescent response, we can estimate blood  $p\text{CO}_2$ . Figure 2 shows a schematic representation of the internal structure of the disposable sensor and its working principle.

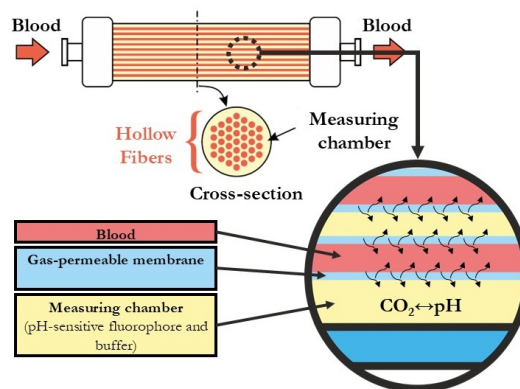


Figure 2. Schematic representation of the internal structure of the disposable sensor and its working principle. The red parts represent the areas through which blood flows; the light blue parts represent the hollow fibers walls; the yellow area is the measuring chamber filled with the sensitive solution. Due to the porosity of the hollow fibers,  $\text{CO}_2$  is exchanged between the fibers and the measuring chamber. The absorbed  $\text{CO}_2$  changes the pH of the sensitive solution and its fluorescent response.

### 2.2. Proposed measuring system: the MS2 system

- The proposed device consists of two main components:
- A DISPOSABLE, LOW-COST FLUORESCENT COMPONENT: it consists of a polycarbonate cuvette housing a bundle of gas-permeable, hydrophobic, and porous polypropylene hollow fibers, shown in Figure 1. The entire module was assembled

in Tecnopolo's "Mario Veronesi" laboratories in Mirandola, Italy. This research center specialises in developing and validating biomedical systems and is capable of producing hollow fibers from scratch and customizing their characteristics [8].

- **A FIXED OPTICAL HEAD:** Based on optoelectronic technology, this component allows the measurement of fluorescent response and does not come into direct contact with blood. The optical head operates using two light sources, LED1 ( $\lambda_{ex-1} = 405$  nm) and LED2 ( $\lambda_{ex-2} = 465$  nm), each emitting light, which passes through its respective excitation filter (Fex1 and Fex2) to isolate the desired excitation wavelengths. These filtered beams are then directed onto the sensor using two dichroic mirrors: D1 and D2. A photodiode (PD1) measures the optical power of the excitation light from both LEDs. To ensure balanced power measurements at PD1 when switching between LED1 and LED2, an additional filter (Fex3) is used to equalize the intensities. The MS2 disposable emits fluorescent light at  $\approx 520$  nm ( $\lambda_{ems}$ ) in response to excitation, and this fluorescence passes through dichroic mirror D2 to reach photodiode PD2. Before reaching PD2, the emission passes through an emission filter (Fem), which blocks any diffused excitation light. The CAD cross-section of the optical head is shown in Figure 3.

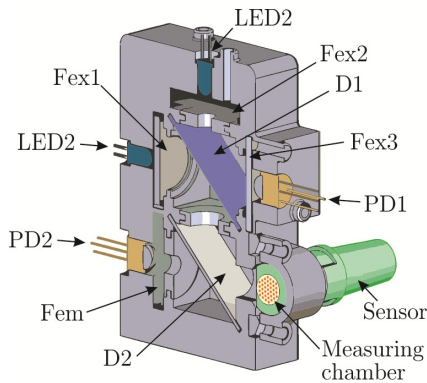
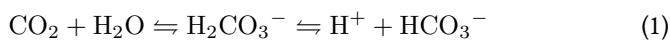


Figure 3. CAD cross-section of the optical head. The figure shows the optoelectronic components and the disposable component (in green).

This configuration enables the system to be integrated directly into the ECC line, eliminating the need for blood sampling procedures. Since the optical head is not in contact with the bloodstream, it remains on board the ECC mainline. Only the disposable sensor requires replacement, which helps reduce contamination risk, overall costs, and plastic waste compared to conventional measurement methods.

### 2.3. Mathematical Model

As stated in Section 2.1., the fibers within the cuvette enable the sensing element to exchange  $\text{CO}_2$  with the patient's blood. Changes in the pH of the sensing solution are linked to  $\text{pCO}_2$  fluctuations through the following chemical reaction:



This gas-permeable membrane ensures equilibrium between the  $\text{pCO}_2$  of the sensing solution and that of the patient's blood under steady-state conditions. As a result, the sensor readings reflect pH changes in the HPTS solution, which in turn correspond to fluctuations in  $\text{pCO}_2$ . The relationship between pH and  $\text{pCO}_2$  is expressed as [12]:

$$[\text{H}^+] = \zeta \cdot \text{pCO}_2 \Rightarrow \text{pH} = -\log_{10}(\zeta \cdot \text{pCO}_2), \quad (2)$$

where  $\zeta$  accounts for i) the solubility coefficient of  $\text{CO}_2$  in the buffer, ii) the first dissociation constant of  $\text{H}_2\text{CO}_3^-$ , and iii) the

concentration of  $\text{HCO}_3^-$  in the sensing element. Once equilibrium is reached, the pH in the measurement chamber is determined by the blood's  $\text{pCO}_2$  in the extracorporeal circuit. Therefore, by monitoring the pH, the  $\text{pCO}_2$  of the blood can be inferred. The  $\text{pCO}_2$  estimation is based on calculating the ratio of the fluorescence emission from the fluorophore solution under excitation by  $\lambda_{ex-1}$  and  $\lambda_{ex-2}$ . The optical head measures fluorescence intensity at  $\lambda_{ems}$  as voltage signals. For each LED, the intensity of the fluorescence emitted by the sensing solution ( $V_{ems}$ ) is corrected for dark ( $V_{dark}$ ) and normalized against the intensity of the excitation radiation from the LED (estimated by the photodiode PD1,  $V_{exc}$ ). The ratio is given by:

$$R = \frac{I_{405}}{I_{465}}, \quad (3)$$

where  $I_{405}$  and  $I_{465}$  are defined as:

$$I_{405} = \frac{V_{ems405} - V_{dark}}{V_{exc405} - V_{dark}}, \quad (4)$$

$$I_{465} = \frac{V_{ems465} - V_{dark}}{V_{exc465} - V_{dark}}$$

In equation 4,  $V_{ems405}$  and  $V_{exc405}$  are the voltages detected by PD2 and PD1, respectively, when LED1 is on;  $V_{ems465}$  and  $V_{exc465}$  are the corresponding voltages when LED2 is on.

The emission voltage ( $V_{ems}$ ), measured by PD2, and the excitation voltage ( $V_{exc}$ ), measured by PD1, depend on the fluorescence intensity, which is pH-sensitive, and the characteristics of the electronic circuitry. The emission signal reflects the optical power of the fluorophore and it is directly related to the target analyte concentration, while the excitation signal compensates for LED intensity fluctuations. The dark signal ( $V_{dark}$ ) accounts for both electrical and optical noise.

As demonstrated in previous works [10] [13] [14], the ratiometric signal is related to the pH of the fluorescent indicator. Assuming that phosphate-buffered saline (PBS) in the measuring chamber maintains the pH near the indicator's  $\text{pK}_a$  (approximately 7.3), the pH is linearly related to the ratio  $R$ :

$$\text{pH} = \alpha' \cdot R + \beta'. \quad (5)$$

Hence, by combining equations (2) and (5), the  $\text{pCO}_2$  in blood can be estimated as:

$$\text{pCO}_{2\text{-est}} = f(R) = \alpha \cdot 10^{-\beta \cdot R} + \gamma, \quad (6)$$

### 2.4. The commercial device: the PreSens system

As previously mentioned, this study also investigates the possibility of off-label use of a commercial sensor not approved for use with blood. Specifically, the commercial optical  $\text{pCO}_2$  sensing system consisting of the PreSens multi-channel MCR-O1P1C1 and SP-CD1  $\text{CO}_2$  sensor spot was analysed. The system is based on optoelectronic sensing technology. The excitation light with a wavelength of 470 nm ( $\lambda_{exc}^P$ ), as specified in the Technical Data Sheet, is transmitted via an optical fiber to the sensing element, which incorporates a fluorescent indicator, as can be observed in Figure 4. Upon excitation, the indicator emits light through a fluorescence emission process, with an experimentally observed emission wavelength of approximately 602 nm ( $\lambda_{ems}^P$ ). The emitted light is then guided back through the same optical fiber to the optical detection unit, where it undergoes signal processing and analysis.

The sensor is designed to measure the partial pressure of  $\text{CO}_2$  ( $\text{pCO}_2$ ) within a range of [8, 190] mmHg, as reported in the manufacturer's specifications. The signal acquisition and data

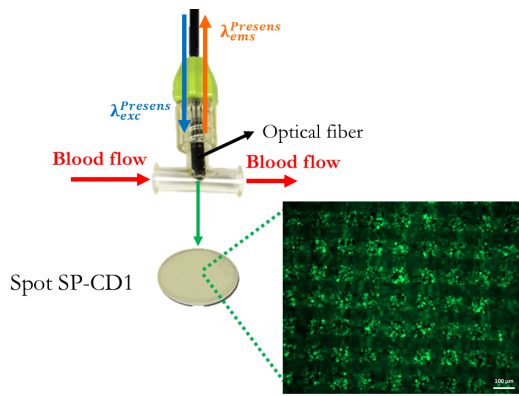


Figure 4. Schematic representation of the working principle of the PreSens sensor. The excitation light ( $\lambda_{exc}^P = 470$  nm) is guided to the CO<sub>2</sub> spot through an optical fiber. The SP-CD1 spot contains a deposited fluorescent indicator, as shown on the right side of the picture. This indicator responds to the excitation by emitting light in turn ( $\lambda_{em}^P = 602$  nm). The emission signal is then driven back to the optical head where it is processed to evaluate the pCO<sub>2</sub>.

processing system is based on a validated patented technology (Patent No.: US 6,602,716 B1), ensuring high precision and reliability across a range of experimental conditions.

A critical aspect of this sensing system is that the sensitive element must remain in direct contact with the target fluid throughout the measurement process. While this design choice supports strong metrological performance, it introduces potential concerns regarding biocompatibility, particularly when the measurand is a complex biological fluid such as whole blood. Direct exposure of the sensor to blood components may lead to undesired interactions, including protein adsorption, clot formation, or sensor fouling, which could compromise both sensor performance and patient safety over time. It is therefore essential to emphasize that the PreSens system is not intended for use with human blood. While this device has been employed in various biological fluid monitoring applications, there is currently no documented or validated use for blood gas monitoring, and its use in such a context must be considered as *off-label*.

The direct contact between sensing spot and blood thus represents a potential biocompatibility risk, which must be carefully considered during experimental design and interpretation of results. Hence, this study aims to assess the sensor's behaviour in presence of blood to evaluate its potential use in contexts where biocompatibility is not required, such as during the development and testing of medical devices. This approach could enable real-time, continuous monitoring of device performance, reducing reliance on sampling alone and analysis with a blood gas analyzer.

## 2.5. Experimental verification

Prior to initiation of the experimental verification, the MS2 sensor was calibrated following the procedure described in [15]. For the PreSens sensor, the calibration coefficients specific to the SP-CD1 CO<sub>2</sub> sensor unit used (supplied by the manufacturer) were entered into its management software.

Then, to evaluate the performance of MS2 and PreSens sensors for blood pCO<sub>2</sub> measurement, an *ex-vivo* test was conducted using bovine blood over a simulated ~ 6.5-hour ECC treatment. Blood was circulated and maintained at a constant temperature of 36.8 °C, while pCO<sub>2</sub> levels were varied within the range [10, 120] mmHg using an oxygenator (Eurosets, Italy) supplied with a controlled mixture of compressed air, CO<sub>2</sub>, and nitrogen (N<sub>2</sub>), as illustrated in Figure 5. A heat exchanger (chiller) was used to ensure thermal stability throughout the experiment.

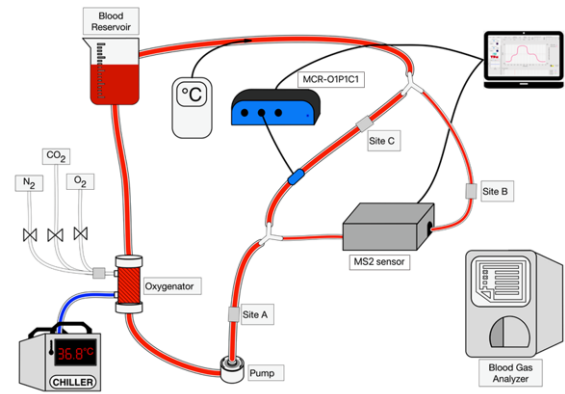


Figure 5. Schematic representation of the blood circuit employed during the experimental acquisition. The flow of N<sub>2</sub>, CO<sub>2</sub> and air through the oxygenator allowed modulation of pCO<sub>2</sub> levels in blood. A constant blood temperature of 36.8 °C and a flow rate of 1.0 L/min were regulated by a chiller and a centrifugal pump. Blood samples were taken from sites A, B and C and analysed with the blood gas analyzer.

In its current prototype stage, the MS2 sensor supports only a limited blood flow. To replicate realistic ECC conditions without exceeding the sensor's mechanical limits, a bypass line was introduced, as shown in Figure 5, allowing only the amount of blood the sensing module could safely tolerate. This design prevented excessive pressure buildup that could compromise the structural integrity of the sensor.

To obtain a rough estimate of the sensor's dynamic response, blood pCO<sub>2</sub> was varied significantly more rapidly than typically observed in clinical ECC scenarios. During these transients, sensor readings were recorded at different sampling frequencies: 0.3 Hz for the MS2 sensor and 0.2 Hz for the PreSens sensor. The resulting measurements were compared with reference pCO<sub>2</sub> values obtained from blood samples analysed using a GEM PREMIER 4000 blood gas analyzer (Werfen, Italy). Sampling was performed at three access points in the circuit, denoted as sites A, B, and C, corresponding to the location of blood gas analyzer, the MS2 sensor, and the PreSens sensor, respectively. During the experimental sessions,  $N = 15$  pCO<sub>2</sub> measurements were obtained using the blood gas analyzer. The resulting values were then compared with those obtained from the sensors under investigation to assess their accuracy and reliability. The experimental conditions for the *ex vivo* test are summarized in Table 1.

Ex vivo test conditions	
Blood type	Bovine blood
Blood temperature	36.8 °C
Test duration	~ 6.5 hours
Blood nominal flow	1.0 L/min
Sampling period MS2 system	0.3 Hz
Sampling period PreSens system	0.2 Hz
Number of blood samples	15

Table 1. *Ex vivo* test conditions employed during the measurement session.

## 2.6. Sites variability

As previously mentioned, due to the more complex internal hydraulic design of the MS2 sensor compared to the PreSens sensor, a bypass line was implemented within the blood circuit, as previously described in Section 2.5.. To ensure that the MS2 sensor would not be exposed to mechanical stress or risk of rupture, and that the modified setup would not introduce hemodynamic

disturbances in blood flow, we conducted a validation using multiple sampling sites. Specifically, blood samples were collected from three distinct sites and analysed for pCO<sub>2</sub> using a blood gas analyzer:

- **Site A** served as the reference point on the main circuit line.
- **Site B** connected to the MS2 sensor line.
- **Site C** connected to the PreSens sensor line.

A schematic of the bypass configuration and sampling sites is shown in Figure 6.

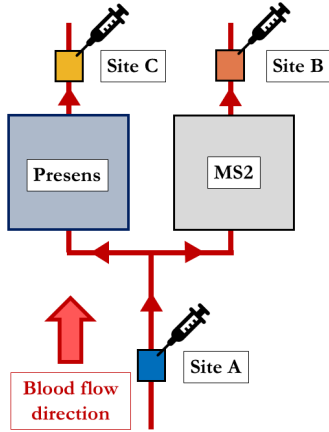


Figure 6. Schematic representation of the bypass line and the sampling sites.

The variability among the three sites, was assessed considering all pCO<sub>2</sub> values collected during the measurement session ( $N = 15$ ).

### 3. RESULTS AND DISCUSSION

In this section, we first discuss the variability across different sampling sites (Section 3.1.). Then, the calibration procedure and the results obtained from the MS2 sensor are presented and compared with the reference values from the blood gas analyzer (Section 3.2.). A similar analysis is carried out for the PreSens sensor in Section 3.3.. Finally, in Section 3.4., we compare the pCO<sub>2</sub> measurements from both sensors with the values obtained from the blood gas analyzer.

#### 3.1. Sites variability

The trend of pCO<sub>2</sub> values collected at the three sites is reported in Figure 7. It can be observed that the blood pCO<sub>2</sub> values

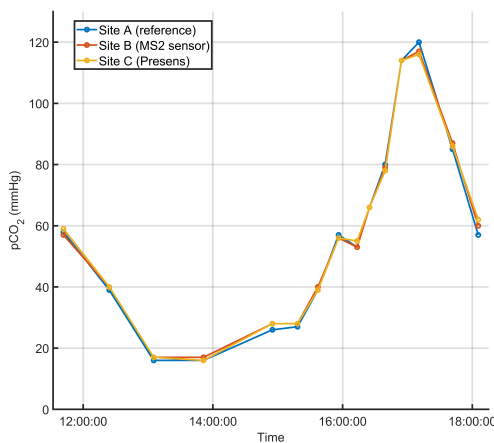


Figure 7. pCO<sub>2</sub> values acquired from the blood gas analyzer at site A (blue line), Site B (orange line) and Site C (yellow line) at 15 different times.

sampled by the blood gas analyzer at each site exhibit similar behaviour and appear to be in good agreement. We also calculated

the experimental standard deviation of the sample for each triad of points, the maximum value obtained is:

$$\sigma_{\max} (\text{mmHg}) = 2.5 \text{ mmHg}$$

which in percentage is:

$$\sigma_{\max} (\%) = 4.2 \%$$

In conclusion, despite the different internal hydraulic structures, we can conclude that the blood pCO<sub>2</sub> inside both sensors is not significantly different.

#### 3.2. MS2 sensor compared with blood gas analyzer

As previously described in Section 2.3., for the MS2 sensor, the estimation of pCO<sub>2</sub> is based on the mathematical model reported in Equation 6. Prior to the measurement session, a calibration procedure was necessary to determine the model parameters  $\alpha$ ,  $\beta$ , and  $\gamma$ ; they were determined by a comparison with a blood gas analyzer. The estimated pCO<sub>2</sub> values measured by the MS2 sensor ( $\text{pCO}_{2-\text{est}}^{\text{MS2}}$ ), during the *ex vivo* test, along with the corresponding reference values ( $\text{pCO}_{2-\text{ref}}^{\text{SiteB}}$ ) obtained from the standard blood gas analyzer, are presented in Figure 8. The raw data were corrected using the mathematical model described by Equation 6.

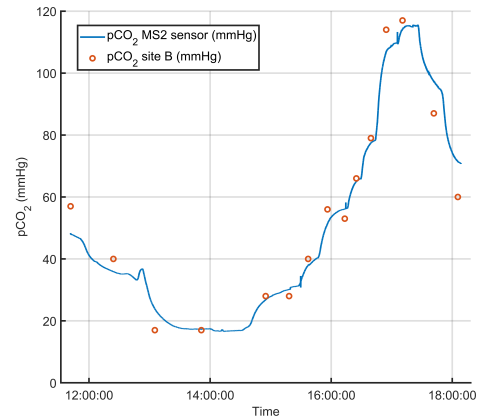


Figure 8.  $\text{pCO}_{2-\text{est}}^{\text{MS2}}$  values measured during the *ex vivo* test (blue line) and the corresponding  $\text{pCO}_{2-\text{ref}}^{\text{SiteB}}$  (red dots) measured by the blood gas analyzer at site B.

As shown, the estimated values are in good agreement with the reference measurements. The measurement error was evaluated using the following equation:

$$\Delta \text{pCO}_2^{\text{MS2}} = \text{pCO}_{2-\text{ref}}^{\text{SiteB}} - \text{pCO}_{2-\text{est}}^{\text{MS2}} \quad (7)$$

Considering a maximum acceptable clinical error of  $\pm 5$  mmHg, Figure 9 reports these errors as calculated from Equation 7 at the 15 different times.

As illustrated, when changes in blood pCO<sub>2</sub> occur rapidly, the error exceeds the  $\pm 5$  mmHg tolerance.

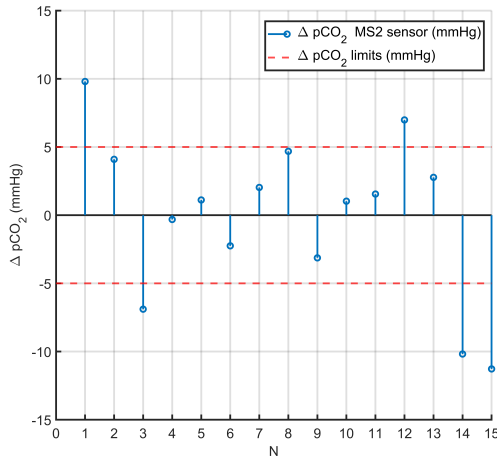


Figure 9. Errors obtained by calculating  $\Delta pCO_2^{MS2}$  (blue line). The red dashed lines show the upper and lower limit of tolerance of  $\pm 5$  mmHg.

We also evaluated the average root mean square error (RMSE) between the measurements provided by the blood gas analyzer and those obtained from the MS2 sensor:

$$RMSE_{avg}^{MS2} = 5.7 \text{ mmHg}$$

which exceeds the considered threshold. This can be attributed to the time required for the sensor to reach equilibrium with the blood, indicating a limitation in its response time and the presence of dynamic error. However, such rapid and large variations are unlikely to occur in clinical practice, as they do not reflect typical patient physiology. It is also important to note that the sensor's response time depends on the exchange surface area. Increasing this surface area, such as by incorporating additional fibers, could accelerate the sensor response and reduce dynamic errors.

### 3.3. PreSens sensor compared with reference system

Figure 10 shows the blood  $pCO_2$  measured by the PreSens sensor compared with reference values obtained from a blood gas analyzer at site C.

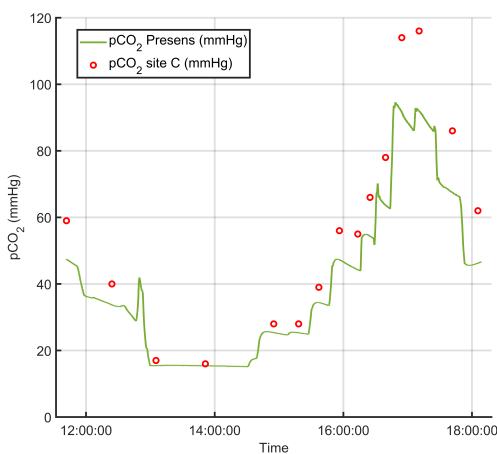


Figure 10.  $pCO_2$  raw data (green line) measured by the PreSens sensor compared with the blood gas analyzer values sampled at site C (red dots).

The sensor raw data generally follow the same trend as the reference instrument. However, despite being calibrated using the manufacturer-provided parameters, the PreSens sensor consistently underestimated the actual  $pCO_2$  values. This prompted an investigation into the presence of a systematic offset and gain

error. This is likely due to the off-label use of the device. For this reason, a data adjustment was performed using 15 reference measurements acquired from the blood gas analyzer at site C to correct this discrepancy. The resulting adjustment allowed us to estimate the linear correction parameters  $a$  (gain) and  $b$  (offset). The correction was applied according to the following equation:

$$pCO_2^{SiteC} = a \cdot pCO_2^P + b \quad (8)$$

In Figure 11 the results of the linear fit adjustment are reported: the offset value ( $b$ ) and the gain ( $a$ ) obtained from the fit, together

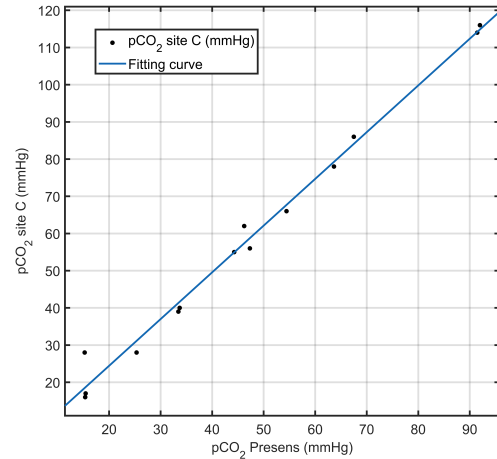


Figure 11. Fitting curve obtained from  $pCO_2$  values of Site C by the blood gas analyzer and the  $pCO_2$  raw data from PreSens sensor.

with the RMSE, are reported in Table 2.

Linear fit parameters	
$a$	1.2562
$b$	-0.6897
RMSE	3.6144

Table 2. Fitting parameters and RMSE from the adjustment procedure.

The PreSens  $pCO_2$  raw data shown in Figure 10 were corrected using the parameters obtained by the linear fit adjustment procedure reported in Table 2. Figure 12 shows the PreSens  $pCO_2$  values after correction.

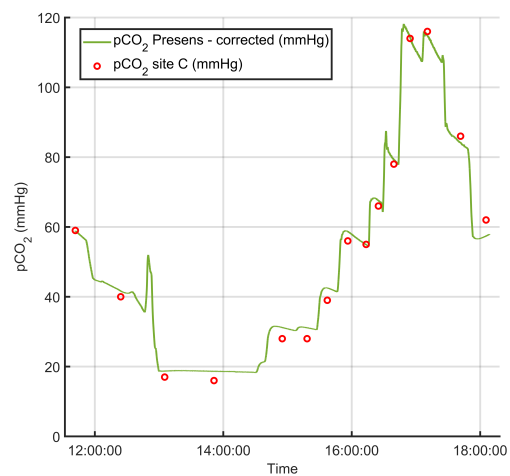


Figure 12. Graph representing the PreSens  $pCO_2$  values corrected (green line) and the blood gas analyzer values measured at site C (red dots).

We can observe that the corrected data are in good agreement with the blood gas analyzer values.

The measurement error before ( $\Delta p\text{CO}_2^{\text{P-pre}}$ ) and after the adjustment ( $\Delta p\text{CO}_2^{\text{P-post}}$ ) procedure were evaluated using the following equations:

$$\Delta p\text{CO}_2^{\text{P-pre}} = p\text{CO}_2^{\text{SiteC}} - p\text{CO}_2^{\text{P-pre}} \quad (9)$$

where  $p\text{CO}_2^{\text{P-pre}}$  represents the PreSens raw data before the adjustment procedure.

$$\Delta p\text{CO}_2^{\text{P-post}} = p\text{CO}_2^{\text{SiteC}} - p\text{CO}_2^{\text{P-post}} \quad (10)$$

where  $p\text{CO}_2^{\text{P-post}}$  represents the PreSens corrected data after the adjustment procedure. Figure 13 shows the measurement errors calculated with Equation 9 and 10 between the blood gas analyzer values collected in Site C and the recalculated  $p\text{CO}_2$  values and the maximum clinical error accepted ( $\pm 5$  mmHg).

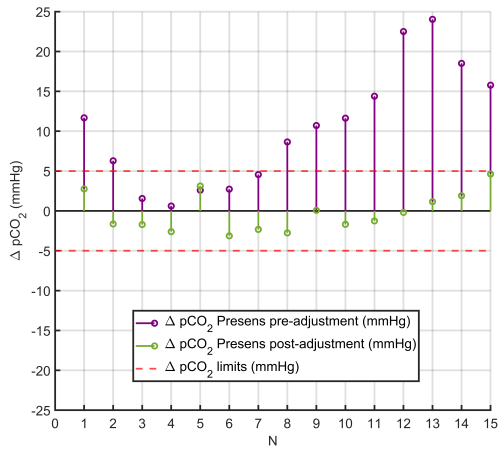


Figure 13. Errors obtained by calculating  $\Delta p\text{CO}_2^{\text{P-pre}}$  (purple line) and  $\Delta p\text{CO}_2^{\text{P-post}}$  (green line). The red dashed lines show the upper and lower limit of tolerance of  $\pm 5$  mmHg.

It is possible to observe that the PreSens values before the adjustment procedure rarely remain within the threshold limits, it seems that PreSens tends to underestimate the  $p\text{CO}_2$  values. As for the PreSens values after the adjustment procedure, all values are inside the maximum threshold. The average RMSE of PreSens values before and after the adjustment procedure between the pairs of points were evaluated:

$$\text{RMSE}_{\text{avg}}^{\text{P-pre}} = 12.7 \text{ mmHg}$$

$$\text{RMSE}_{\text{avg}}^{\text{P-post}} = 2.5 \text{ mmHg}$$

The adjustment procedure led to a significant improvement in PreSens performance, reducing the measurement error by 80.5%. Hence, the PreSens sensor appears suitable for *ex vivo* testing, provided that a calibration-based correction procedure is applied.

### 3.4. Curves comparison

To conclude the analysis, we compared the  $p\text{CO}_2$  curves obtained from the MS2 sensor and the PreSens sensor. Figure 14 illustrates the comparison between the two datasets. The curves show good agreement with each other and with the reference values provided by the blood gas analyzer. The correlation coefficient between the two curves was calculated as

$$r = 0.96$$

indicating a very strong correlation [16] and good consistency between the MS2 and PreSens sensors with respect to the blood gas analyzer reference.

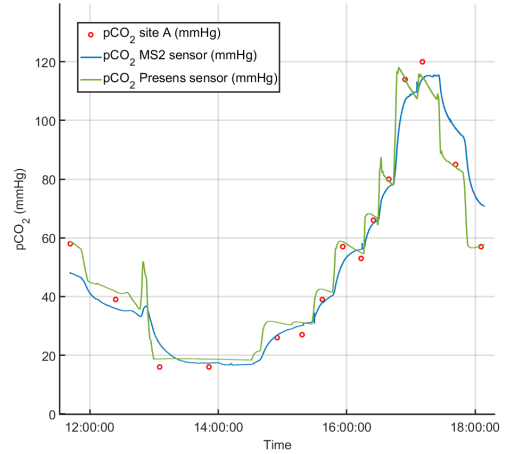


Figure 14. Comparison between the  $p\text{CO}_2$  curves of the MS2 sensor (in blue) and the PreSens sensor (green) after correction. The red dots are the  $p\text{CO}_2$  values measured at site A.

## 4. CONCLUSIONS

In conclusion, although the limited number of fibers used in the MS2 sensor prototype constrains its dynamic performance, particularly its response and rise time during rapid changes in blood  $p\text{CO}_2$ , the experimental results demonstrate that it can still provide reliable  $p\text{CO}_2$  estimates during ECC. The slower dynamic is likely due to the time required for the sensor to reach equilibrium with the blood. Such abrupt and large  $p\text{CO}_2$  fluctuations are unlikely in real clinical scenarios and therefore do not reflect typical patient monitoring conditions.

The MS2 sensor further benefits from a robust ratiometric detection strategy and the use of hollow fiber technology, which prevents direct contact between the sensing solution and the patient's blood. This design satisfies biocompatibility requirements and supports long-term use, as demonstrated by hollow fibers already employed in ECMO systems.

By contrast, the PreSens sensor, despite being highly responsive and reliable even during rapid  $p\text{CO}_2$  changes, raises potential biocompatibility concerns and requires recalibration, likely due to its off-label use in this experimental setting.

Overall, these findings suggest that the MS2 sensor has strong potential for integration into clinical workflows, offering a safe and biocompatible solution for continuous  $p\text{CO}_2$  monitoring, with the potential to reduce monitoring costs in ECC. The PreSens sensor, on the other hand, may be better suited for applications where biocompatibility is not essential, such as *ex vivo* testing during medical device validation, provided that appropriate calibration adjustments are implemented.

## AUTHORS' CONTRIBUTION

This work was carried out through the joint contribution of several authors. The initial phase, involving the design and development of a new device based on an already validated technology, was conducted by Alessia Gallerani, Alberto Ferrari, and Marco Muzzarelli, with the collaboration of Stefano Cattini, who provided the technology and the necessary know-how for the activities. The experimental activities were performed and supported by Alessia Gallerani and Stefano Cattini. The analysis of the experimental data was carried out by Alessia Gallerani, under the supervision of Alberto Ferrari. The overall coordination and scientific supervision of the work were ensured by Professor Luigi Rovati.

## ACKNOWLEDGMENT

We would like to thank Dinamica Generale S.p.A., Poggio Rusco (MN), Italy, for supporting the experimental activities.

## REFERENCES

- [1] J. Marhong, E. Fan, Carbon Dioxide in the Critically Ill: Too Much or Too Little of a Good Thing? *Respiratory Care*, vol. 59, oct 2014, no. 10, p. 1597–1605.  
DOI: [10.4187/respcare.03405](https://doi.org/10.4187/respcare.03405)
- [2] M. C. Frost, M. E. Meyerhoff, Real-Time Monitoring of Critical Care Analytes in the Bloodstream with Chemical Sensors: Progress and Challenges, *Annual Review of Analytical Chemistry*, vol. 8, Jul. 2015, no. 1, p. 171–192.  
DOI: [10.1146/annurev-anchem-071114-040443](https://doi.org/10.1146/annurev-anchem-071114-040443)
- [3] G. Urban, J. Guttman, J. Kieninger, A. Weltin, J. Wöllenstein, J. Zosel, CO<sub>2</sub> sensing in medicine, *Carbon Dioxide Sensing*, Mar. 2019, p. 391–413, ISBN: 9783527688302.  
DOI: [10.1002/9783527688302.ch16](https://doi.org/10.1002/9783527688302.ch16)
- [4] M. Vafaei, A. Amini, A. Siadatan, Breakthrough in CO<sub>2</sub> Measurement With a Chamberless NDIR Optical Gas Sensor, *IEEE Transactions on Instrumentation and Measurement*, vol. 69, May 2020, no. 5, p. 2258–2268.  
DOI: [10.1109/tim.2019.2920702](https://doi.org/10.1109/tim.2019.2920702)
- [5] H. Endoh, T. Honda, S. Oohashi, Y. Nagata, C. Shibue, K. Shimoji, Continuous intra-jugular venous blood-gas monitoring with the Paratrend 7 during hypothermic cardiopulmonary bypass, *British Journal of Anaesthesia*, vol. 87, Aug. 2001, no. 2, p. 223–228.  
DOI: [10.1093/bja/87.2.223](https://doi.org/10.1093/bja/87.2.223)
- [6] D. Howerton, J. M. Krolak, A. Manasterski, J. H. Handsfield, Proficiency Testing Performance in US Laboratories: Results Reported to the Centers for Medicare & Medicaid Services, 1994 Through 2006, *Archives of Pathology & Laboratory Medicine*, vol. 134, may 2010, no. 5, p. 751–758.  
DOI: [10.5858/134.5.751](https://doi.org/10.5858/134.5.751)
- [7] R. D. Dias, L. Kennedy-Metz, G. Rance, R. Srey, R. E. Harari, P. Borges, S. Mendu, P. O’Gara, M. Gombolay, M. Zenati, Monitoring of Perfusionists’ Cognitive Load and Stress and Patients’ Oxygen Delivery during Cardiopulmonary Bypass in Cardiac Surgery, *HSMR 2025*, Imperial College London, 2025, ser. HSMR 2025.  
DOI: [10.31256/hsmr25.93](https://doi.org/10.31256/hsmr25.93)
- [8] A. Gallerani, M. Muzzarelli, G. Gibertoni, A. Ferrari, S. Cattini, L. Rovati, An enhanced measuring instrument for in-line and real-time blood-pco<sub>2</sub> monitoring using a custom-developed gas-exchange filter, *Optical Fibers and Sensors for Medical Diagnostics, Treatment, and Environmental Applications XXV*, SPIE, Mar. 2025, I. Gannot, K. Roodenko (editors), p. 5.  
DOI: [10.1117/12.3041103](https://doi.org/10.1117/12.3041103)
- [9] H. R. Kermis, Y. Kostov, P. Harms, G. Rao, Dual Excitation Ratiometric Fluorescent pH Sensor for Noninvasive Bioprocess Monitoring: Development and Application, *Biotechnology Progress*, vol. 18, Jan. 2002, no. 5, p. 1047–1053.  
DOI: [10.1021/bp0255560](https://doi.org/10.1021/bp0255560)
- [10] S. Cattini, S. Truzzi, L. Accorsi, L. Rovati, Performances and Robustness of a Fluorescent Sensor for Nearly Neutral pH Measurements in Healthcare, *IEEE Transactions on Instrumentation and Measurement*, vol. 69, Oct. 2020, no. 10, p. 7658–7665.  
DOI: [10.1109/tim.2020.2984964](https://doi.org/10.1109/tim.2020.2984964)
- [11] G. Y. Wiederschain, *The Molecular Probes handbook. A guide to fluorescent probes and labeling technologies*: (I. Johnson and M. Spence (eds.) 11th Edition, Life Technologies, 2010, 1060 p., 100), *Biochemistry (Moscow)*, vol. 76, Nov. 2011, no. 11, p. 1276–1276.  
DOI: [10.1134/s0006297911110101](https://doi.org/10.1134/s0006297911110101)
- [12] J. W. Parker, O. Laksin, C. Yu, M. L. Lau, S. Klima, R. Fisher, I. Scott, B. W. Atwater, Fiber-optic sensors for ph and carbon dioxide using a self-referencing dye, *Analytical Chemistry*, vol. 65, Sep. 1993, no. 17, p. 2329–2334.  
DOI: [10.1021/ac00065a027](https://doi.org/10.1021/ac00065a027)
- [13] S. Cattini, L. Accorsi, S. Truzzi, L. Rovati, On the Development of an Instrument for In-Line and Real-Time Monitoring of Blood-pH in Extracorporeal Circulation, *IEEE Transactions on Instrumentation and Measurement*, vol. 69, Aug. 2020, no. 8, p. 5640–5648.  
DOI: [10.1109/tim.2019.2961499](https://doi.org/10.1109/tim.2019.2961499)
- [14] D. Goldoni, A. Ferrari, M. Piccini, S. Cattini, R. Molinari, L. Rovati, Blood-pH Optical Measurement: A Model to Compensate for the Effects of Temperature, *IEEE Transactions on Instrumentation and Measurement*, vol. 72, 2023, p. 1–8.  
DOI: [10.1109/tim.2023.3250282](https://doi.org/10.1109/tim.2023.3250282)
- [15] S. Cattini, S. Truzzi, L. Accorsi, L. Rovati, A Measuring Instrument for In-Line and Real-Time Measurement of Blood-pCO<sub>2</sub> in Extracorporeal-Circulation, *IEEE Transactions on Instrumentation and Measurement*, vol. 70, 2021, pp. 1–9.  
DOI: [10.1109/TIM.2020.3017030](https://doi.org/10.1109/TIM.2020.3017030)
- [16] P. Schober, C. Boer, L. A. Schwarte, Correlation Coefficients: Appropriate Use and Interpretation, *Anesthesia & Analgesia*, vol. 126, May 2018, no. 5, p. 1763–1768.  
DOI: [10.1213/ane.0000000000002864](https://doi.org/10.1213/ane.0000000000002864)